END
DATE
FILMED
1 82
DTIC

1.0

2.8 2.5
3.2 2.2
3.6
4.0 2.0

1.1

1.8

1.25 1.4 1.6

MICROCOPY RESOLUTION TEST CHART
NATIONAL BUREAU OF STANDARDS 1963 A

LEVEL

TR-1084
AFOSR-77-3271

July 1981

SYNTHESIS OF TEXTURES USING
SIMULTANEOUS AUTOREGRESSIVE
MODELS

R. Chellappa

Computer Vision Laboratory
Computer Science Center
University of Maryland
College Park, MD   20742

DTIC
SELECTED
DEC 1 5 1981
H

ABSTRACT

Experimental results of synthesis of some real textures
using a class of spatial interaction models known as simul-
taneous autoregressive (SAR) models are given. The role of
statistical inference methods in texture modeling is empha-
sized.

SECURITY CLASSIFICATION OF THIS PAGE *(When Data Entered)*

REPORT DOCUMENTATION PAGE		READ INSTRUCTIONS BEFORE COMPLETING FORM
1. REPORT NUMBER **AFOSR-TR- 81-0795**	2. GOVT ACCESSION NO. AD-AJC8584	3. RECIPIENT'S CATALOG NUMBER
4. TITLE *(and Subtitle)* SYNTHESIS OF TEXTURES USING SIMULTANEOUS AUTOREGRESSIVE MODELS		5. TYPE OF REPORT & PERIOD COVERED Technical
		6. PERFORMING ORG. REPORT NUMBER TR-1082
7. AUTHOR(s) R. Chellappa		8. CONTRACT OR GRANT NUMBER(s) AFOSR-77-3271
9. PERFORMING ORGANIZATION NAME AND ADDRESS Computer Vision Laboratory Computer Science Center University of Maryland College Park, MD 20742		10. PROGRAM ELEMENT, PROJECT, TASK AREA & WORK UNIT NUMBERS 61102F; 2304/A2
11. CONTROLLING OFFICE NAME AND ADDRESS Math & Info. Sciences, AFOSR/NM Bolling AFB Washington, DC 20332		12. REPORT DATE July 1981
		13. NUMBER OF PAGES 34
14. MONITORING AGENCY NAME & ADDRESS(*if different from Controlling Office*)		15. SECURITY CLASS. *(of this report)* UNCLASSIFIED
		15a. DECLASSIFICATION/DOWNGRADING SCHEDULE

16. DISTRIBUTION STATEMENT *(of this Report)*

Approved for public release; distribution unlimited

17. DISTRIBUTION STATEMENT *(of the abstract entered in Block 20, if different from Report)*

18. SUPPLEMENTARY NOTES

19. KEY WORDS *(Continue on reverse side if necessary and identify by block number)*

Image processing
Pattern recognition
Image models
SAR models
Texture analysis

20. ABSTRACT *(Continue on reverse side if necessary and identify by block number)*

Experimental results of synthesis of some real textures using a class of spatial interaction models known as simultaneous autoregressive (SAR) models are given. The role of statistical inference methods in texture modeling is emphasized.

DD ₁ FORM 73 1473   EDITION OF 1 NOV 65 IS OBSOLETE   UNCLASSIFIED

1. Introduction

Texture is an important characteristic for the analysis of many images. Image texture can be described in terms of a two-level mechanism, one to describe the basic primitives composing the texture and the other to describe the spatial layout of the primitives. The primitives may be of deterministic shape such as squares, circles, hexagons, or may be of completely random shape. Textures such as ceiling tiles and bricks can be grouped under the first category while textures such as grass and sand fall under the second category. It may be possible to model patterns such as bricks and tiles by using the placement rule model [Rosenfeld, Troy, 1970; Zucker, 1974]. Such a description may be very complex for random textures such as cork and grass due to the random shapes and orientations of the primitives.

We take the view that the given texture is generated by an underlying random field characterized by appropriate parametric models. One of the prime characteristics of this approach is that the models considered for the textures are generative, i.e., given the structure of the model and reasonable estimates of the parameters characterizing the model synthetic textures close to the original textures may be obtained. Several generative stochastic models are known in the literature for texture analysis. By appending the successive rows, the resulting image vector has been modeled by seasonal

81 12 14 042

autoregressive and moving average models (ARMA) and their variants [McCormick, Jayaramamurthy, 1974], and by seasonal autoregressive models [Delp, et al., 1979]. Since we are dealing with two-dimensional textures, intuitively it would be preferable to represent the textures using 2-D models. Two-dimensional causal ARMA models have been suggested for textures in [Tou, 1980]. However, the causal models are only a restricted set of models.

Recently, a different class of spatial interaction models known as conditional Markov (CM) models have been used for modeling textures [Hassner, Sklansky, 1978A; 1978B; 1980; Cross, 1980]. Hassner and Sklansky [1978A; 1978B] have pointed out the equivalence between the Gibbs field and Markov random field and generated some synthetic binary textures. The coding method [Besag, 1974] for obtaining the estimates of the CM models has been briefly mentioned. Cross [1980] has generated a wide variety of binary and eight-level synthetic textures using the Monte Carlo simulation procedure [Metropolis, Rosenbluth, et al., 1953]. The Monte Carlo procedure is iterative in nature and involves considerable computational time for generating synthetic textures with large numbers of gray levels.

Our main emphasis in this paper is to illustrate the appropriateness of SAR models for textures. Although under Gaussian situations, there exists a correspondence between the classes

of SAR and CM models [Besag, 1974] in that given a SAR model,
an equivalent CM model can be found, this correspondence
is true only in second-order properties. Hence for non-
Gaussian situations, the two models are different. In the
equivalent SAR and CM models, usually the SAR models are
characterized by a lesser number of parameters. The main
attraction of the SAR models considered here is that the
methods can be easily generalized to non-Gaussian situations.
Such a generalization to non-Gaussian situations using CM
models is unattractive due to the computationally expensive
iterative schemes used for synthesis [Cross, 1980].

The organization of this paper is as follows: In Section
2, we give the theoretical variograms of several SAR models.
Many of these variograms exhibit periodic patterns found in
the variograms of natural textures. Section 3 discusses the
role of statistical inference methods in texture modeling
using SAR models. Specifically, we review the role of spe-
cific estimation methods and model selection rules discussed
in [Chellappa, 1980; Chellappa, Kashyap, 1981B; Chellappa,
1981]. In Section 4, we give the experimental results of
fitting SAR models to cork, grass, wood, sand and paper taken
from Brodatz's album [Brodatz, 1956]. The quality of fit is
evaluated using visual inspection and empirical variograms
of the reconstructed textures. Finally, a brief discussion is
given in Section 5.

2. Appropriateness of SAR models for texture synthesis

We intend to illustrate the usefulness of SAR models for textures in two steps, using the synthetic patterns generated by known SAR models and the theoretical variograms of SAR models. In an earlier report [Chellappa, 1980], several synthetic patterns were generated using SAR models. Contrary to the existing belief [Modestino, et al., 1979] that spatial interaction models such as SAR models are incapable of exhibiting local replication attributes, an essential ingredient of texture, several of the synthetic patterns generated by the SAR models do show local replication.

Another way of judging the appropriateness of SAR models is by using the variogram. Suppose $\{y(s), s \in \Omega\}$, $\Omega = \{s=(i,j), 1 \le i, j \le M\}$ are the observations from the texture. Then the variogram at displacement (k, ℓ) is defined as

$$V(k, \ell) = E[[y(s) - y(s+(k, \ell))]^2]$$
$$= 2R_{0,0}\{1-\rho_{k,\ell}\} \qquad (2.1)$$

where $\rho_{k,\ell}$ is the normalized autocorrelation function. An expression for the theoretical variogram may be obtained by assuming that the given set of observations $\{y(s)\}$ obeys a finite lattice SAR model in (2.2)-(2.3) [Kashyap, 1980A; 1980B; 1981]. Prior to that we partition the finite lattice Ω into two sets Ω_I and Ω_B, defined below:

$$\Omega_B = \{s=(i,j): \; s\in\Omega \text{ and } (s+r)\in\Omega\}$$

and

$$\Omega_I = \Omega - \Omega_B$$

The representation of $\{y(s)\}$ is different in Ω_I and Ω_B as given below:

$$y(s) = \sum_{\gamma\in N} \theta_\gamma \; y(s+\gamma) + \sqrt{\beta}\omega(s), s\in\Omega_I \qquad (2.2)$$

and

$$y(s) = \sum_{\gamma\in N} \theta_\gamma y_1(s+\gamma) + \sqrt{\beta}\omega(s), s\in\Omega_B \qquad (2.3)$$

where

$$y_1(s+(k,\ell)) \quad \text{with} \quad s=(i,j)$$

$$= y(s+(k,\ell)) \quad \text{if} \quad (s+(k,\ell))\in\Omega$$

$$= y[(i+k-1)\bmod M+1, \; (j+\ell-1)\bmod M+1] \text{ if}$$

$$(s+(k,\ell))\notin\Omega.$$

In (2.2) and (2.3), $\{\omega(.)\}$ is an independent and identically (IID) distributed noise sequence. The set N is known as the neighbor set, and depending upon the specific choice of N, causal, semicausal and noncausal models are obtained [Jain, Jain, 1978]. Causal or more generally unilateral neighbor sets are finite subsets of the half plane S^+ defined in [Goodman, Ekstrom, 1980]. The observation set $\{y(s)\}$ is not Markov with respect to N, i.e.,

$$p(ys)|\text{all } y(\gamma), \; \gamma\neq s)$$

$$\neq p(y(s)|\text{all } y(s+\gamma), \; \gamma\in N) \qquad (2.4)$$

as is true for CM models.

Due to the specific finite lattice representation, the normalized autocorrelation function $\rho_{k,\ell}$ at lag (k,ℓ) can be written as [Chellappa, Kashyap, 1981A]

$$\rho_{k,\ell} = \frac{\sum_{s \in \Omega} \exp \sqrt{-1} \, \lambda_0 [(s-\underset{\sim}{1})^T (k,\ell)] / ||\mu_s||^2}{\sum_{s \in \Omega} 1 / ||\mu_s||^2} \tag{2.5}$$

where

$$\mu_s = (1 - \underset{\sim}{\theta}^T \underset{\sim}{\psi}_s), s \in \Omega, \lambda_0 = \frac{2\pi}{M} \tag{2.6}$$

$$\underset{\sim}{\psi}_s = \text{Col.}[\exp(\sqrt{-1}(s-1)^T \gamma), \gamma \in N] \tag{2.7}$$

and

$$\underset{\sim}{1} = (1,1)^T$$

The variograms $V(k,\ell)$ related to $\rho_{k,\ell}$ as in (2.1) are plotted in Figure 1 for several SAR models. The details of the models are given in Table 1. For each model we have plotted variograms along the four directions $(0,i),(i,0),(i,i),(i,-i)$ in a discrete lattice. The structure of the possible variograms with two-dimensional SAR models is quite varied and many of them possess oscillatory behavior, a characteristic of the variograms of natural textures with periodic patterns [Schacnter, et al., 1978].

3.   Statistical inference methods in texture modeling

Before a SAR model can be fitted to the given texture,
two problems have to be tackled: a method for determining
the structure of the "best" SAR model and a method of esti-
mating the parameters of the model given the structure
of the model. For SAR models with unilateral neighbor sets
the classical least square (LS) estimates are consistent
and efficient for the Gaussian case but the LS estimates
are not consistent for nonunilateral neighbor sets [Ord,
1975; Kashyap, Chellappa, 1981]. To obtain consistent and
efficient estimates, maximum likelihood (ML) estimates can
be obtained by making appropriate assumptions regarding the
distribution of $\{\omega(s)\}$. Due to the Jacobian of the trans-
formation matrix from $\{\omega(.)\}$ to $\{y(.)\}$ not being unity for
non-unilateral neighbor set SAR models, the log likelihood
function for Gaussian $\{y(s)\}$ is non-quadratic in the para-
meters. This requires the use of computationally expensive
gradient schemes like Newton-Raphson to obtain ML estimates.
An iterative scheme with reduced computations has been deve-
loped in [Chellappa, 1980; Chellappa, Kashyap, 1981B;
Cnellappa, 1981] which yields approximate ML estimates. The
approximate ML estimates $\overline{\theta}, \overline{\beta}$ are obtained as limits of
θ_{t+1}, β_t given below:

$$\underset{\sim}{\theta}_{t+1} = (\underset{\sim}{R} - \frac{1}{\beta_t} \underset{\sim}{S})^{-1} (\underset{\sim}{V} - \frac{1}{\beta_t} \underset{\sim}{U}), t=0,1,2,3,\ldots, \qquad (2.8)$$

$$\beta_t = \frac{1}{M^2} \sum_{\Omega} (y(s) - \underset{\sim}{\theta}_t^T \underset{\sim}{z}(s))^2, \quad t=0,1,2,3,\ldots \tag{2.9}$$

where

$$\underset{\sim}{S} = \sum_{\Omega} \underset{\sim}{z}(s)\underset{\sim}{z}^T(s), \quad m \times m \text{ matrix} \tag{2.10}$$

$$\underset{\sim}{U} = \sum_{\Omega} \underset{\sim}{z}(s)y(s), \quad m \times 1 \text{ vector} \tag{2.11}$$

$$\underset{\sim}{V} = \sum_{\Omega} \underset{\sim}{C}_s, \quad m \times 1 \text{ vector} \tag{2.12}$$

$$\underset{\sim}{R} = \sum_{\Omega} (\underset{\sim}{S}_s \underset{\sim}{S}_s - \underset{\sim}{C}_s \underset{\sim}{C}_s^T), \quad m \times m \text{ matrix} \tag{2.13}$$

$$\underset{\sim}{C}_s = \text{Col.}[\cos \frac{2\pi}{M}(s-\underset{\sim}{1})^T \underset{\sim}{\gamma}, \gamma \in N]$$

and

$$\underset{\sim}{S}_s = \text{Col.}[\sin \frac{2\pi}{M}(s-\underset{\sim}{1})^T \underset{\sim}{\gamma}, \gamma \in N]$$

The initial value $\underset{\sim}{\theta}_0$ is chosen as follows:

$$\underset{\sim}{\theta}_0 = \underset{\sim}{S}^{-1}\underset{\sim}{U}.$$

All the summations in (2.8)-(2.13) are over $s \in \Omega$ and
m is the dimension of $\underset{\sim}{\theta}$. The use of approximate ML
estimates in texture modeling has been emphasized in [Chellappa,
1980; Chellappa, Kashyap, 1981B] using synthetic patterns.
The quality of the regenerated synthetic textures using
approximate ML estimates is better than the synthetic tex-
tures using inconsistent LS estimates.

Thus far in our discussions we have assumed that the
underlying structure N of the model is known. In practice,
the appropriate N is to be estimated from the given texture
data. Asymptotically consistent, transitive and parsimonious
decision rules to choose the appropriate N for the given

texture have been given in [Chellappa, 1980; Kashyap, Chellappa, 1981]. The derivation of these decision rules may be found in [Kashyap, et al., 1981]. The relevance of these decision rules in texture modeling has been illustrated in [Chellappa, 1980; Kashyap, Chellappa, 1981] using synthetic patterns. Several SAR models were fitted to the data generated by a known SAR model and the test statistic g_n given in (2.14) was computed for each model:

$$g_n = M^2 \log \overline{\beta}_n - \sum_{s \in \Omega} \log (1 - 2\overline{\theta}_n^T C_{sn}$$

$$+ \overline{\theta}_n^T Q_{sn} \overline{\theta}_n) + 2M_n \log M \tag{2.14}$$

where

$$Q_{sn} = (\sum_{s \in \Omega} C_{sn} C_{sn}^T + S_{sn} S_{sn}^T) \tag{2.15}$$

The model corresponding to the minimum of g_n is chosen as the appropriate model. This decision rule correctly eliminates several inappropriate models. One way of judging the inappropriateness of a model is by evaluating the quality of the synthetic texture generated by the model. The synthetic textures corresponding to clearly inappropriate models are not similar to the original. But the synthetic patterns corresponding to SAR models whose neighbor sets include the neighbor set of the true model are very similar to the original making visual judgment subjective. Due to its preference for parsimonious models, the decision rule minimizing g_n correctly eliminates the over-parameterized models.

4. Real texture synthesis using SAR models

Our discussions so far have been concerned with synthetic image patterns generated by known SAR models. The next step is to investigate the appropriateness of SAR and CM models for natural textures like sand, cork, grass, etc. For our experiments, we chose 5 textures from Brodatz's album [1956]. The 64×64 textures selected were cork, sand, grass, wood and paper. We report the results of fitting SAR models to the textures mentioned above as a sequence of experiments.

In the first experiment, different SAR models were fitted to cork using the estimation scheme in (2.8)-(2.9). The details of the fitted models are in Table 2; the estimate $\bar{\beta}$ and the test statistic g_n in (2.14) are in Table 3. The patterns corresponding to the fitted models, generated using a Gaussian pseudo-random number generator, are given in Figure 2. The synthetic textures (1,2),(1,3), and (2,1) corresponding to SAR models N_{S1}, N_{S2}, and N_{S3} are not good. In fact, models N_{S1} and N_{S2} give non-stationary patterns. The quality of the synthetic textures (2,2)-(3,2) is significantly improved when neighbors farther than the nearest are included, as in models N_{S4} through N_{S7} in Table 2. Since the reduction in variance is not significant by increasing the number of parameters from 10 to 14, the decision statistic g_n for the 10 parameter model N_{S4} is less than those for the 12 and 14 parameter models N_{S6} and N_{S7}. However, the 18 parameter model

N_{S7} is preferred to the lower order models. Observe that the patterns corresponding to the last four models are very similar.

The synthetic cork textures corresponding to models N_{S4} - N_{S7} display the diagonal pattern present in the original cork. However, the synthetic textures seem to have more abrupt variations in their intensities than the original cork, i.e., distinct dark and white patches are present in the synthetic textures rather than smooth variations as in the original cork.

Note that the synthetic textures in Figure 2 were generated using a Gaussian pseudo-random number generator. Better quality can be achieved if the noise sequence used to generate the synthetic textures is derived by using the histogram of the actual residuals. The actual residuals $\{\bar{\omega}(.)\}$ were produced by using

$$\bar{\omega} = \frac{1}{\beta}[H(\bar{\theta})\underline{y} - \bar{\alpha}\underline{1}] \tag{2.16}$$

where $\bar{\beta}, \bar{\theta}$ and $\bar{\alpha}$ are the estimates of β, θ, and α, respectively. We used three standard programs BDCOU1, MDGC and GGVCR from the IMSL package in that order to generate a set of random deviates whose histogram approximates the histogram of the exact residuals. The exact residuals were tallied into twenty bins using BDCOU1. The normalized frequencies obtained from BDCOU1 were fed as inputs to MDGC. The cumulative distribution function of the residuals obtained from MDGC was used to

generate the required random deviates. The results of synthetic generation using the histogram matched random numbers are given in Figure 3. Figure (1,1) is the original cork texture, and window (1,2) is the synthetic texture using the 14 parameter SAR model and Gaussian random number generator. The synthetic texture using the histogram matched residuals is in window (1,3).

The results of fitting SAR models to the other textures under consideration are given in Figure 4. The model fitted was 14 parameter SAR model N_{S6} and histogram matched residuals were used to generate the synthetic textures. The synthetic paper texture (1,2) in Figure 4 retains the vertical directionality present in the original in (1,1). As mentioned before, some large patches not in the original texture are present in the synthetic image. The horizontal streak-like pattern present in the original wood texture (2,1) is reasonably picked up in the synthetic wood (2,2), with a few additional patches. The synthetic grass (2,3) corresponding to the natural grass in (1,3) is not as good as cork or wood. This is probably due to the fact that grass appears to be more inhomogenous compared to cork or wood. As in the case of paper and cork the directionality present in sand (3,1) is picked up in the synthetic texture (3,2). Another way of judging the quality of texture synthesis is to see if the second order properties such as the variogram, etc. of the synthetic texture

are close to the original data. To answer this query, variograms of original textures and synthetic textures are given side by side in Figure 5. The synthetic textures correspond to SAR model N_{S6} and were generated using histogram matched residuals. Note that in all the cases the variograms of synthetic textures are reasonably similar to the original variograms. One that is worthy of pointing out is the variogram of the synthetic wood along $(0,i)$.

It is probable that a 64×64 data set may be large for a 14 parameter model. Large images may be blocked into small images and each block may be modeled separately [Delp, et al., 1979]. The results of fitting 12 parameter symmetric SAR models to 32×32 blocks of four textures, cork, sand, paper, and grass, are given in Figure 6. The synthetic textures were constructed using histogram matched residuals. Compared to the 64×64 synthetic cork texture, the 32×32 synthetic cork in window (2,2) has fewer abrupt intensity variations. The sand and paper textures also show such results. However, the 32×32 synthetic grass (1,4) is not as good as the 64×64 synthetic grass in Figure 6.

5. Discussion

We have given some experimental results of our attempts to synthesize a class of real textures. The textures considered belong to the class of microtextures. There have been several earlier attempts to synthesize real textures, notably the work reported by Cross [1980] and Garber and Sawchuck [1981]. Cross considered a wider class of textures than attempted in our study. In the Monte Carlo procedures used for synthesis purposes, the size of the state set increases rapidly with the number of gray levels. Hence, to avoid excessive computations, two and eight level images obtained by an equal probability quantization procedure [Haralick, et al., 1973] have been fitted with CM models. Coding estimates have been used to generate synthetic textures. Good results have been reported for the textures considered in our study. It has been concluded that CM models are poor fits to textures such as brick, water, and wood. It is not clear if the bad fits are due to inefficient coding estimates or due to the distinctly inhomogeneous structure of wood, water and brick due to the reduction in number of gray levels or due to the inadequacy of the CM models themselves. Our limited experiments with SAR models have given reasonably good results for wood and it appears that much larger parameter sets are required for water. Due to the extremely

high regularity present in the brick, probably a two-stage procedure may be appropriate [Cross, 1980, p. 137]. In the first stage we can model the line patterns for bricks and subsequently fill in the areas using a SAR model.

A number of synthesis techniques have been suggested in [Garber, Sawchuck, 1981] for binary and gray level textures. Mostly unilateral models have been considered compared to the more general SAR models used in our study. Consequently, LS estimates have been used to generate synthetic images. No quantitative rules are available in their study for choosing an appropriate model. Good results have been reported for binary images and some gray level images. Better results might have been obtained on smaller images since the number of parameters required would be much smaller leading to better accuracy in estimation.

Table 1. Details of SAR Models Whose Variograms
are in Figure 1. β is assumed to 1.1111.

Model Identification	$\underline{N}$	Parameter $\underset{\sim}{\theta}$
Fig. 1a	$(-1,0),(-1,1),(0,1),(1,1)$	$\theta_{-1,0}=.18, \theta_{-1,1}=-.1806$
		$\theta_{0,1}=1.1011, \theta_{1,1}=-1.0390$
Fig. 1b	$(-1,0),(-1,1),(0,1),(1,1)$	$\theta_{-1,0}=\theta_{1,0}=.5256$
	$(1,0),(1,-1),(0,-1),(-1,-1)$	$\theta_{-1,1}=\theta_{1,-1}=-.2480$
		$\theta_{0,1}=\theta_{0,-1}=.5081$
		$\theta_{1,1}=\theta_{-1,-1}=-.2876$
Fig. 1c	$(-1,0),(0,-1),(-1,-1),$	$\theta_{-1,0}=1.0388,$
	$(-2,0),(0,-2)$	$\theta_{0,-1}=.9046$
		$\theta_{-1,-1}=-.7288$
		$\theta_{-2,1}=-.1804, \theta_{0,-2}=$
		$-.1048$
Fig. 1d	$(-1,0),(-1,1),(0, 1)$	$\theta_{-1,0}=\theta_{1,0}=.28,$
	$(1,0),(1,-1),(0,-1)$	$\theta_{0,-1}=\theta_{0,1}=-.14$
		$\theta_{-1,1}=\theta_{1,-1}=.22$

Table 1
(cont.)

Model Identification	$\underline{N}$	Parameter $\underset{\sim}{\theta}$
Fig. 1e	$(-1,0),(0,-1),(-1,-1)$	$\theta_{-1,0}=.9704,$ $\theta_{0,-1}=.9735,$ $\theta_{-1,-1}=-.9686$
Fig. 1f	$(-1,1),(0,1),(1,1)$ $(1,-1),(0,-1),(-1,-1)$	$\theta_{-1,1}=\theta_{1,-1}=.23,$ $\theta_{0,1}=\theta_{0,-1}=-.14$ $\theta_{1,1}=\theta_{-1,-1}=.22$

Table 2

Symmetric neighbor sets of SAR
models fitted to cork

Model Number	Symmetric Neighbor Set
N_{S1}	$(0,1),(1,0)$
N_{S2}	$(0,1),(1,0),(1,-1),(-1,-1)$
N_{S3}	$(0,1),(1,0),(1,-1),(-1,-1),(0,2),(2,0)$
N_{S4}	$(0,1),(1,0),(1,-1),(1,1),(0,2),(2,0)$ $(-2,1),(2,1),(1,2),(-1,2)$
N_{S5}	$N_{S4} \cup \{(2,2),(-2,2)\}$
N_{S6}	$N_{S5} \cup \{(3,0),(0,3)\}$
N_{S7}	$N_{S6} \cup \{(1,3),(3,1),(-1,3),(-3,1)\}$

Table 3

Estimate $\overline{\beta}$ and test statistics g_n for SAR models
fitted to cork. Variance of data = 714.04

Model Number	$\overline{\beta}$	g_n
N_{S1}	200.02	Non-stationary
N_{S2}	169.78	Non-stationary
N_{S3}	168.52	23423.0
N_{S4}	157.73	23225.0
N_{S5}	157.68	23243.0
N_{S6}	157.71	23257.0
N_{S7}	155.28	23207.0

(a)   (b)
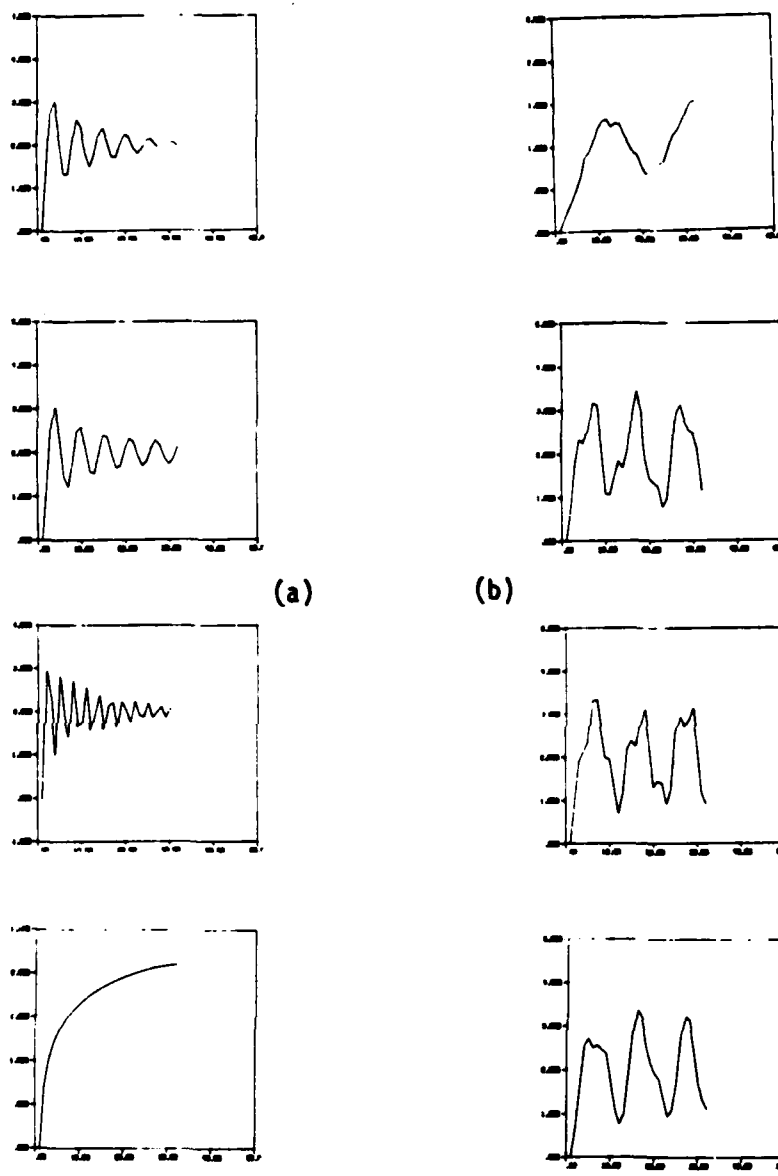
Figure 1.   The theoretical variograms of the SAR
            models in Table 1. V(0,k) versus k
            is plotted in the first row, V(k,0)
            versus k in the second row , V(k,k)
            versus k in the third row and V(k,-k)
            versus k in the fourth row.
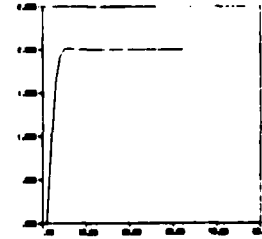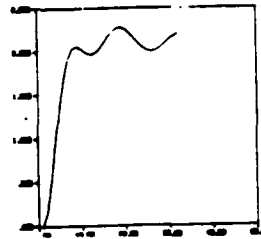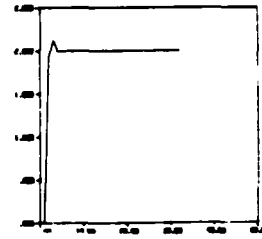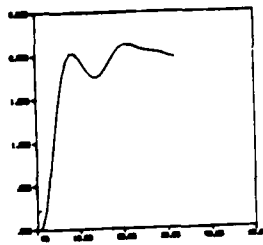
(c)　　　(d)
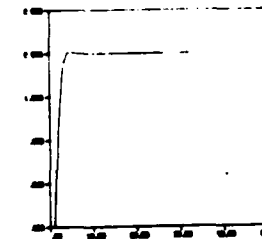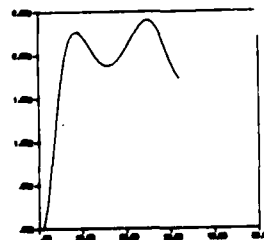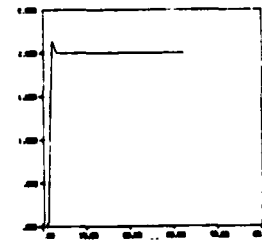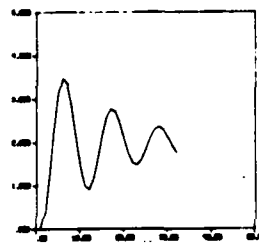
Figure 1(cont'd.)
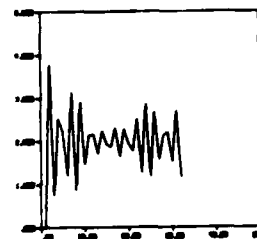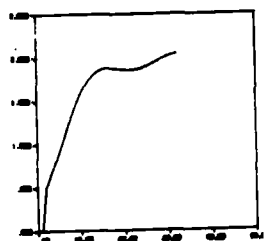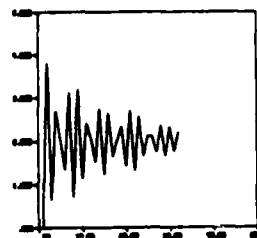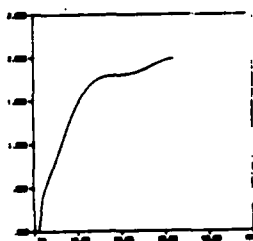
(e)   (f)
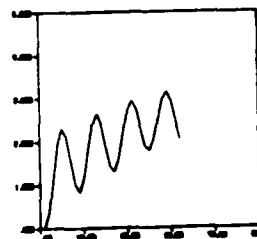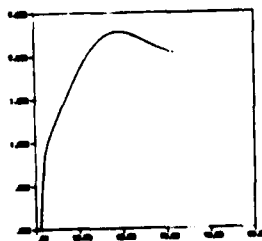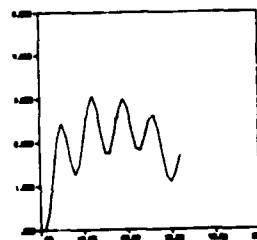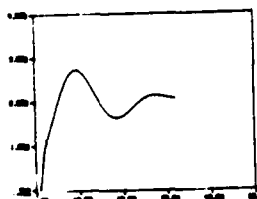
Figure 1 (cont'd.)
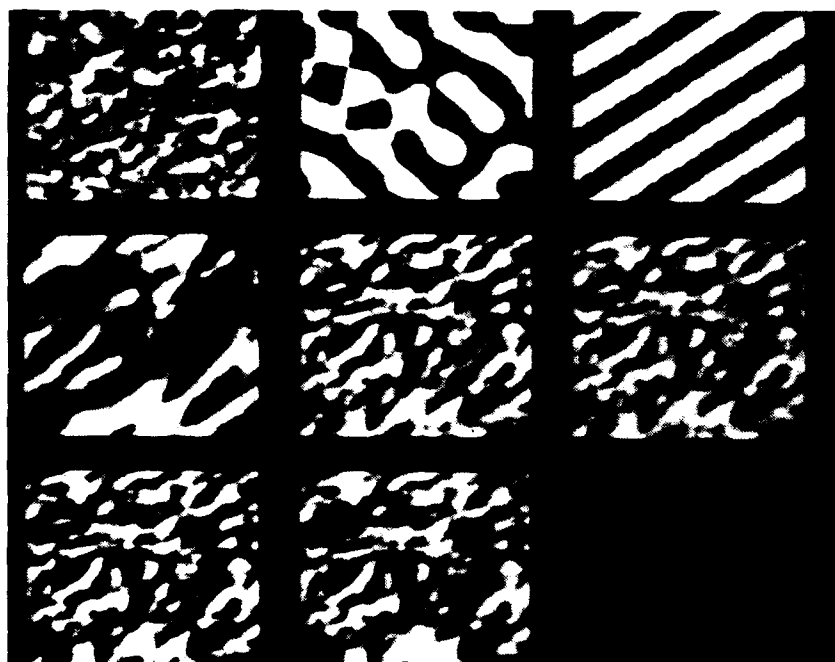
Figure 2. Synthesis of cork texture using SAR models.
(1,1) is the original cork, (1,2),(1,3),(2,1)
were generated by models N_{S1} - N_{S3} of Table 2.
Patterns (2,2),(2,3),(3,1) and (3,2) were
generated by N_{S4} - N_{S7}.
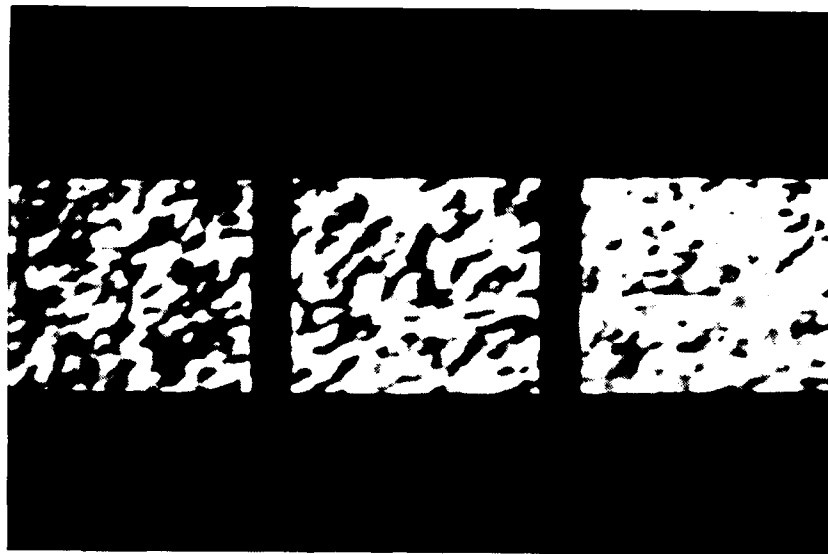
Figure 3.   Results of using histogram matched residuals.
(1,1) is original cork, (1,2) was generated by
N_{S6} of Table 2 using Gaussian pseudorandom
numbers and (1,3) was generated by N_{S6} and
histogram matched residuals.
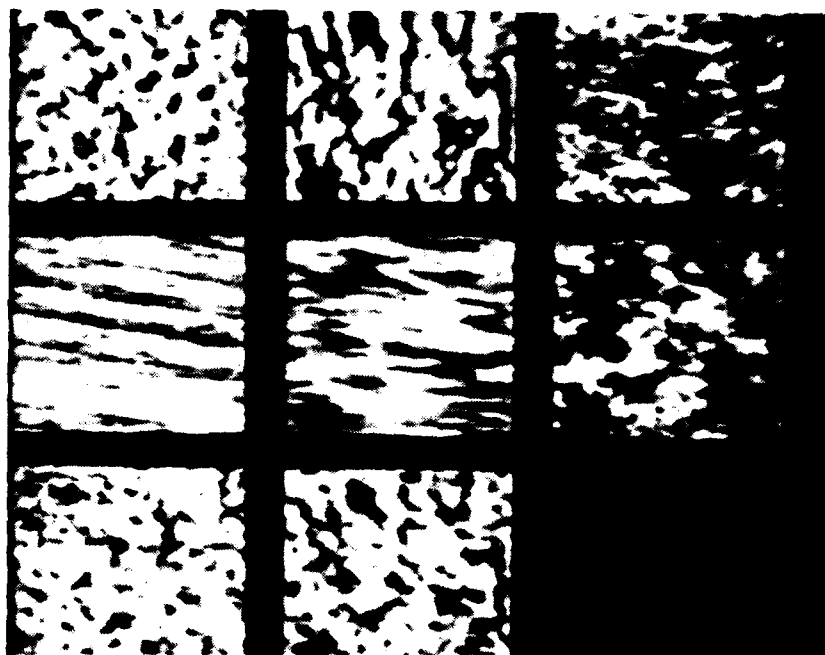
Figure 4. Results of fitting SAR models to other textures.
All the synthetic textures were generated using
N_{S6} and histogram matched residuals.

(1,1) and (1,2): original and synthetic paper.
(1,3) and (2,3): original and synthetic grass.
(2,1) and (2,2): original and synthetic wood.
(3,1) and (3,2): original and synthetic sand.
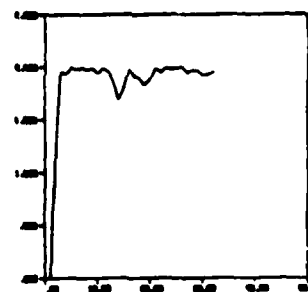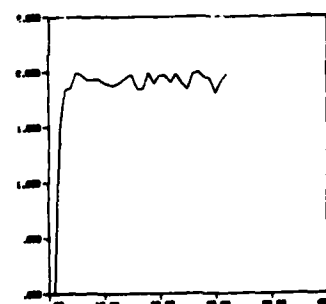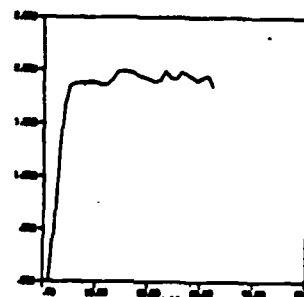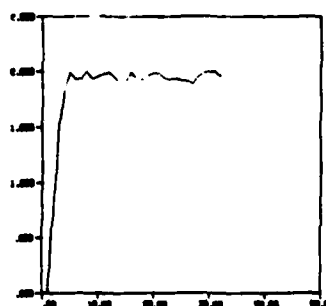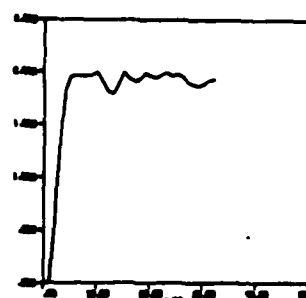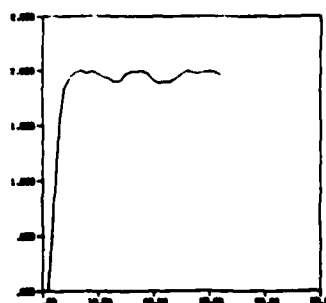
Original Cork   Synthetic Cork

Figure 5. Variograms of natural and synthetic textures. Synthetic textures were generated using SAR model N_{S6} and histogram matched residuals.
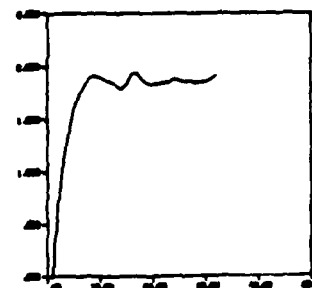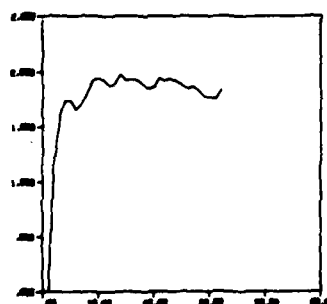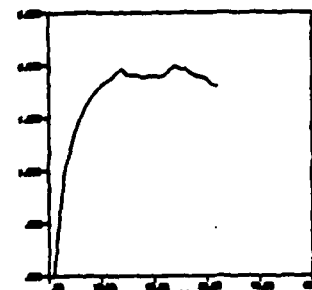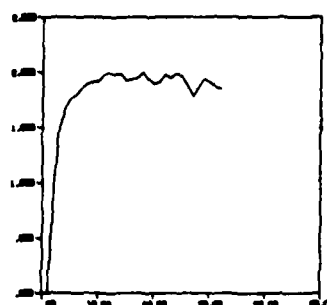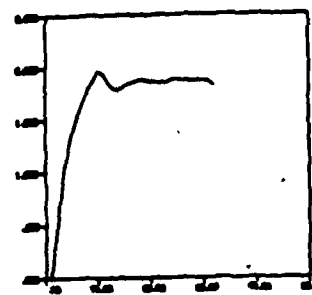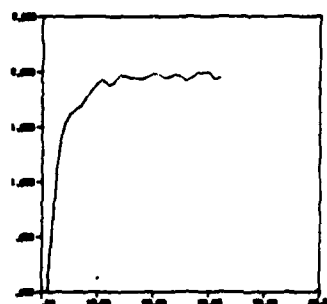
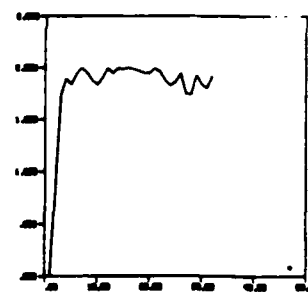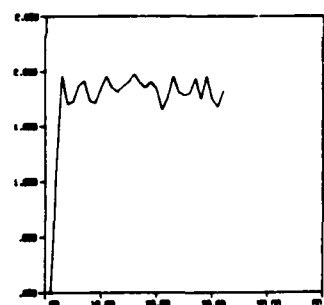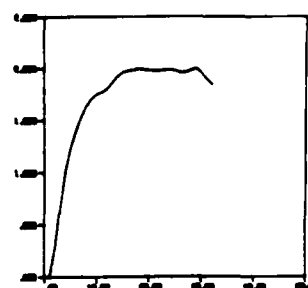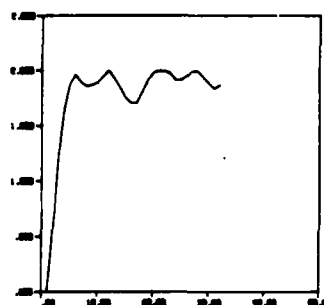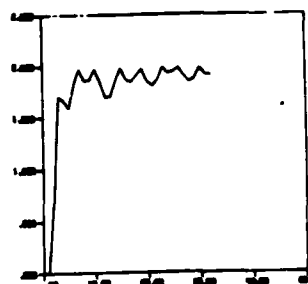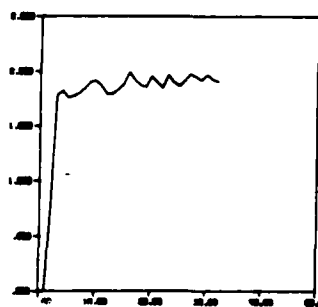Original grass   Synthetic grass

Figure 5 (cont'd.)
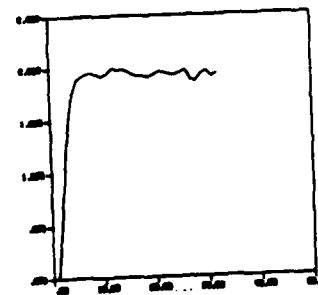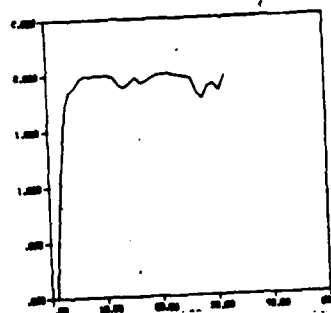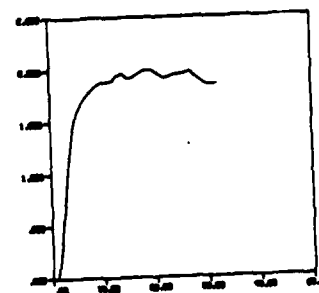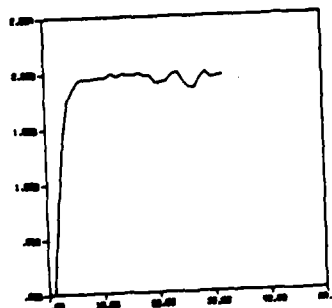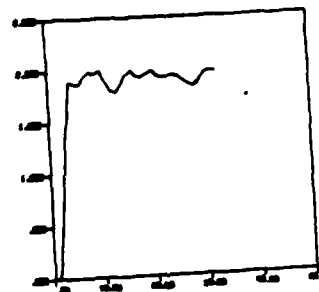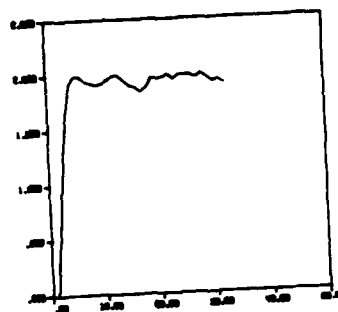
Original sand

Synthetic sand

Figure 5 (cont'd.)

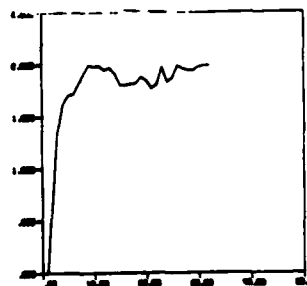Original paper   Synthetic paper

Figure 5 (cont'd.)
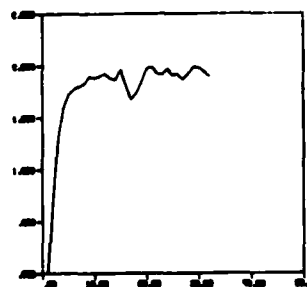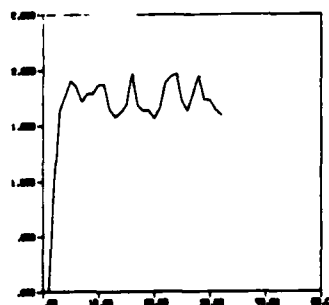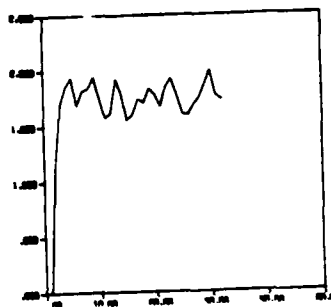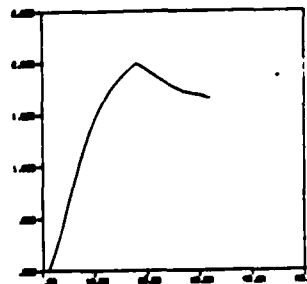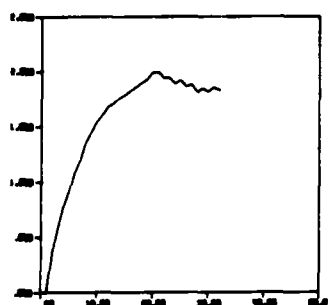
Original wood   Synthetic wood

Figure 5 (cont'd.)
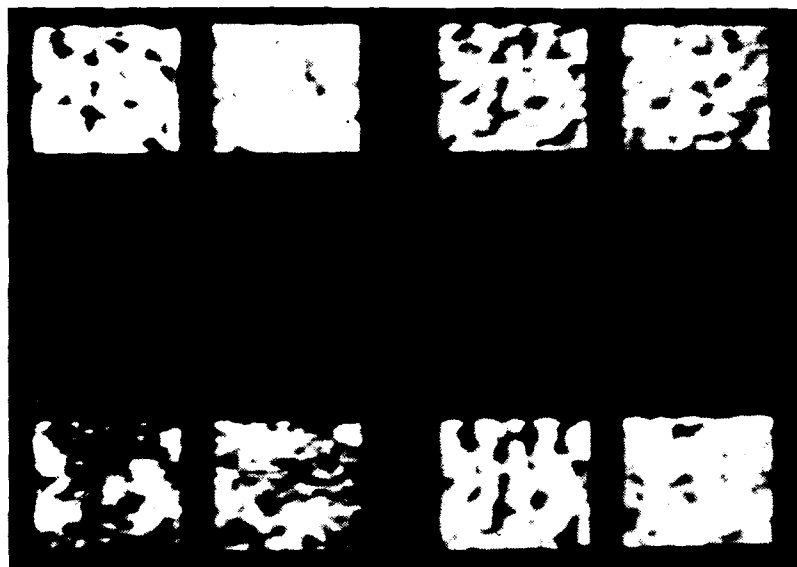
Figure 6. Results of fitting SAR models to
32×32 blocks of textures. All the synthetic
textures were generated using N_{SS} and
histogram matched residuals. (1,1) and
(1,2): original and synthetic paper.
(1,3) and (1,4): original and synthetic
grass. (2,1) and (2,2): original and
synthetic cork. (2,3) and (2,4): original
and synthetic sand.

References

1. Besag, J. E. (1974). "Spatial interaction and statistical analysis of lattice systems," Jl. Royal Stat. Soc., Ser. B, Vol. B-36, pp. 192-236.

2. Brodatz, P. (1956). Textures: A Photographic Album for Artists and Designers, New York: Dover.

3. Chellappa, R. (1980). "Fitting random field models to images," Tech. Report TR-928, Computer Science Ctr., University of Maryland, College Park, MD, August.

4. Chellappa, R., and Kashyap, R. L. (1981A). "On the correlation structure of random field models of textures," Proc. of IEEE Computer Society Conf. on Pattern Recognition and Image Processing, Dallas, TX, August.

5. Chellappa, R. and Kashyap, R. L. (1981B). "Synthetic generation and estimation in random field models of images," Proc. of IEEE Computer Society Conf. on Pattern Recognition and Image Processing, Dallas, TX, August.

6. Chellappa, R. (1981). "Stochastic models in image analysis and processing," Ph.D. thesis, Purdue University, August.

7. Delp, E. J., Kasnyap, R. L., and Mitchell, O. R. (1979). Image data compression using autoregressive time series models," Pattern Recognition, Vol. 11, pp. 313-323, December.

8. Garber, D. D. and Sawchuck, A. A. (1981). "Computational models for texture analysis and synthesis," in Proc. of Image Understanding Workshop, pp. 69-88, April.

9. Goodman, D. M. and Ekstrom, M. P. (1980). "Multi-dimensional spectral factorization and unilateral AR models," IEEE Trans. Automatic Control, Vol. AC-25, pp. 258-262, April.

10. Haralick, R. M., Shanmugam, K. and Dinstein, I. (1973). "Textural features for image classification," IEEE Trans. Syst., Man, Cybern., Vol. SMC-3, pp. 610-621, November.

11. Hassner, M., and Sklansky, J. (1978A). "Markov random fields as models of digitized image texture," Proc. IEEE Computer Society Conf. on Pattern Recognition and Image Processing, 1978, pp. 346-351, June.

12. Hassner, M., and Sklansky, J. (1978B). "Markov random field models of digitized image texture," Proc. 4th Int. Conf. on Pattern Recognition, pp. 538-540, November.

/

13. Hassner, M., and Sklansky, J. (1980). "The use of Markov random fields as models of textures," Computer Graphics and Image Processing, Vol. 12, pp. 376-406, April.

14. Jain, A. K. and Jain, J. R. (1978). "Partial difference equations and finite difference methods in image processing - Part 2: image restoration," IEEE Trans. Automatic Control, Vol. AC-23, pp. 817-833, October.

15. Kashyap, R. L. (1980A). "Univariate and multivariate random field models for images," Computer Graphics and Image Processing, Vol. 12, pp. 257-270, March.

16. Kashyap, R. L. (1980B). "Random field models on finite lattices for finite images," Proc. of 5th Intl. Conf. on Pattern Recognition, Miami, FL, December.

17. Kashyap, R. L. (1981). "Random field models on finite lattices for finite images," Presented at the Conference on Information Sciences, Johns Hopkins University, May.

18. Kashyap, R. L. and Chellappa, R. (1981). "Estimation and choice of neighbors in spatial interaction models of images " (submitted for publication).

19. Kashyap, R. L., Chellappa, R., and Ahuja, N. (1981). "Decision rules for the choice of neighbors in random field models of images," Computer Graphics and Image Processing, Vol. 15, pp. 301-318, April.

20. McCormick, R. H. and Jayaramamurthy, S. N. (1974). "Time series models for texture synthesis," Int. Jl. Comput. Inform. Sci., Vol. 3, pp. 329-343, December.

21. Metropolis, N., Rosenbluth, A. W., Rosenbluth, M. N., Teller, A. H., and Teller, E. (1953). "Equations of state calculations by fast computing machines," J. Chem. Phys., Vol. 21, pp. 1087-1092.

22. Modestino, J. W., Fries, R. W., and Vickers, A. L. (1979). "Texture discrimination based upon an assumed stochastic texture model," Tech. Report TR-79-3, Electrical and Systems Eng. Dept., Rennselaer Polytechnic Institute, Troy, NY, July.

23. Ord, K. (1975). "Estimation methods for models of spatial interaction," Jl. Amer. Stat. Assn., Vol. 70, pp. 120-126, March.

24. Rosenfeld, A. and Troy, E. (1970). "Visual texture analysis," Tech. Report TR-116, Computer Science Ctr., University of Maryland, College Park, MD, June.

25. Schachter, B., Rosenfeld, A., and Davis, L. S. (1978). "Random mosaic models for textures," IEEE Trans. Syst., Man, Cybern., Vol. SMC-8, pp. 694-702, September.

26. Tou, J. T. (1980). "Pictorial feature extraction and recognition via image modeling," Computer Graphics and Image Processing, Vol. 12, pp. 376-406, April.

27. Zucker, S. W. (1976). "On the foundations of texture: A transformational approach," Tech. Report TR-331, Computer Science Ctr., University of Maryland, College Park, MD, September.

DAT FILM